

**THE SIMULATION STUDY OF GNSS SIGNAL REFLECTION IN
MONITORING SEA LEVELS AND TSUNAMI**

**Buldan Muslim¹⁾, Mokhammad Nur Cahyadi²⁾, Bambang Sunardi³⁾ and
Charisma Juni Kumalasari³⁾**

¹*National Institute of Aeronautics and Space (LAPAN), Bandung 40173, Indonesia*

²*Department of Geomatics Engineering, Institut Teknologi Sepuluh Nopember Kampus ITS
Sukolilo, Surabaya, 60111, Indonesia*

³*Mathematics Department, Master's Programme, Institut Teknologi Sepuluh Nopember,
Surabaya 60111, Indonesia*

Corresponding author: mbuldan@gmail.com

ABSTRACT

A real-time Global Navigation Satellite System (GNSS) data managed by the Geospatial Information Agency (BIG) can be developed for indirect tsunami monitoring. This involves using GNSS TEC data due to the atmospheric-ionosphere coupling through tsunami-triggered infrared waves. The application of this method is, however, limited to tsunamis originating from earthquake epicenter which is far from the coast. Meanwhile, the arrival

Vol 39 No. 4, page 192 (2020)

of tsunamis to the coast requires a longer time than the propagation of infrasound waves into the ionosphere. This GNSS signal reflection technique can, therefore, be used to detect tsunamis which are close to shore in order to overcome the detection weakness associated with the GNSS TEC and also routinely used to monitor sea waves. This research conducted a simulation of this technique using single-frequency code distance data to determine the sea level and the results showed its effectiveness in determining sea wave height using one differentiation. It is also possible to ignore the difference in the bias of two receivers of direct and reflected signals by sea-level assuming they are similar and have identical antennas. The use of pseudo distance from the GNSS signal code data makes it possible to estimate the height of the sea waves by simulation with a standard deviation of approximately 5.6 cm.

Keywords: GNSS, Signals, Reflections, Sea Levels, Tsunamis

1. INTRODUCTION

Sea level monitoring is an important concept in understanding several aspects of hydrosphere such as local hydrodynamics, tidal wave activity, and others. It is also related to the weather due to the ability of typhoons to cause major damage in coastal areas in extreme conditions and greater damage associated with tsunamis. Therefore, the Meteorology Climatology and Geophysics Council (BMKG) builds and operates a tsunami early warning system motivated by the Aceh earthquake and tsunami of December 26, 2004 (Harijono et al. 2010).

Tides are a natural phenomenon defined as the periodic rise and fall of sea levels due to the gravitational forces of celestial bodies, especially the moon and the sun. The influence of other astronomical objects can, however, be ignored due to their relatively smaller distance and size compared to the moon and sun. Meanwhile, the non-astronomical factors influencing tides, especially in semi-closed waters such as bays, are the shape of the coastline and the bottom topography of the waters (R.H. Stewart. 2008).

Sea level is monitored conventionally by tidal devices which measure the vertical distance of the water surface from the point of observation. Several countries operate tidal observation networks to monitor changes in sea level due to the ability of the measurement tools to provide precise and accurate results. The installation of these devices, however, requires direct contact with water and this limits their frequent use and maintenance. Moreover, the equipment is very vulnerable to coastal hazards such as coastal flooding and tsunamis thereby causing measurement errors and damage during the extreme natural phenomenon. They also require expensive regular maintenance, especially due to the need of divers (Artru et al. 2005).

GNSS has the ability to function as an alternative approach to sea level monitoring, especially due to some signals received through reflections from a surface near the antenna which are called multipath (Artru et al. 2005). This, therefore, means there is possibility of using the multipath technique for tidal monitoring and, unlike the devices used in measuring sea level near shore, it also has the ability to monitor sea levels far from shore. The extent of sea-level monitoring with GNSS, however, depends on the height of its antenna and the elevation angle of its satellite. Therefore, the GNSS signal reflection technique is also applicable for tsunami monitoring when it is slightly far from the coast.

GNSS has been successfully applied for positioning, navigation, and remote regulation over the past few decades, especially the GNSS-Reflectometry (GNSS-R) which is an innovative sensing technique using GNSS signals reflected from the Earth's surface (Jin et al. 2005 and Zavarot et al. 2014). Its data application for marine altimetry was first proposed by (Martin-Neira. 1993) while Garrison et al. also conducted a study on the reflected signal of the global positioning system (GPS) used for roughness on the reflection surface (Garrison et al. 1998).

In sea-level observations, especially coastal areas, it is usually difficult to use radar altimeters. Moreover, geophysical factor models such as the earth's gravitational field or ocean currents are not sufficient to predict local sea levels and the changes in these levels in the 21st century are usually accompanied by storm surges and extreme flood (Semmling et al. 2012) which are dangerous for the population.

Stosius et al. (2010) conducted a tsunami detection simulation using GNSS-Reflectometry in the Indian Ocean with the focus on six historic tsunami events generated by earthquakes with different magnitudes in several types of constellations and orbit parameters, as well as the GNSS-R carrier phase compared to the PARIS approach or the altimetry code (Peltier and Hines. 1976).

Muslims et al. (2019) also conducted a simulation study using the JOG2 station and the results showed the reflecting point with the ability to reflect GNSS signals and are received at an altitude of about 20 meters from sea level has the furthest distance around 1150 meters from receivers on the beach (Muslim et al. 2019). The tsunami has a speed of 75.2 m/s at a depth of 1000 meters for the coast with a depth of 30 degrees and, assuming a constant speed, it was observed to have reached the coast in 13 seconds. This time is not enough to make people avoid the tsunami based on the early warning system and in order to ensure it is effectiveness, the GNSS signal amplifier antenna is required to be at least 60 m high to produce a 39-second chance of avoiding a tsunami. The study of GPS satellite elevation angles with signal receiver antennas at a height of 20 meters showed the availability of satellites observed in the GPS signal simulation at JOG2 station has an elevation angle lesser than 30 degrees by the sea for almost 24 hours except at 11:00 AM-11:50 AM.

This paper provides a brief overview of the simulations of GPS signal reflections to determine sea level using an IGS station, JOG2, located in Java. The process involved

investigating the sea level estimation using pseudo distance data of GPS code signals at L1 frequency.

2. METHODOLOGY TO DETERMINE THE SEA LEVELS WITH GNSS SIGNAL REFLECTIONS

The absolute sea level height can be obtained based on ITRF using two receivers, RHCP receiver facing upward or peak and LHCP facing sea level or nadir (Rudenko et al. 2019). The RHCP receiver receives signals coming directly from the GNSS satellite and is used to estimate the absolute position of the antenna (Lofgren et al. 2014) while LHCP receivers receive those reflected by the sea level (Chen et al. 2012).

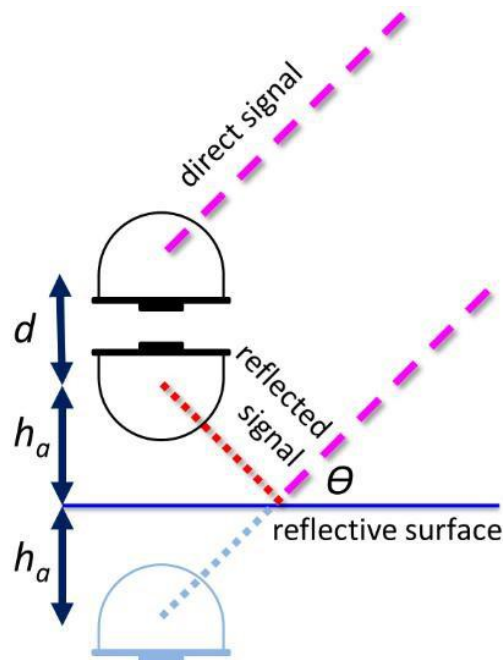


Figure 1. The arrangement of the direct signal receiver antenna as a reference station (above), the reflected signal (below) from the GNSS satellite, and the shadow rover antenna (below sea level).

First, the baseline between RHCP and LHCP antennas needs to be determined to obtain sea-level changes. The arrangement of the direct and reflected signal receiver antenna is, however, explained in Figure 1.

According to the figure, when a nadir antenna receives a signal reflected from the sea

level, it is possible to assume a direct signal below sea level is received with an elevation angle Θ and the reflected signal observed is considered the rover receiver data while the direct signal is considered the reference station data. The equation of the rover antenna position can, therefore, be formulated with an ordinary differential method in order to determine the relative position. In Figure 1, d is the actual distance between the direct and reflected signal receiving antennas while h_a is the sea level height which is the same for the shadow rover receiver below the sea level (Muslim et al. 2019).

A change in the sea level causes a variation in the h_a and the sea level height is directly related to the basic distance between the reference antenna and rover with a geometric relationship.

$$\Delta v = 2h_a + d$$

where:

Δv is the baseline between the RHCP and LHCP antennas

h_a is the distance between the LHCP antenna and sea level

d is the distance between the phase center of the RHCP and LHCP antennas

RHCP and LHCP antennas allow users to change the base and sea levels in the ITRF reference.

2.1 The positioning of shadow rover receiver antenna using phase data

One of the methods used to estimate the position of the shadow rover is the differential method with the GNSS observation equation for two different receivers, A (reference) and B (rover), stated as follows:

$$L_A^j = \rho_A^j + c(\tau_A - \tau^j) + Z_A^j - I_A^j + B_A^j + \epsilon \quad (1)$$

$$L_B^j = \rho_B^j + c(\tau_B - \tau^j) + Z_B^j - I_B^j + B_B^j + \epsilon \quad (2)$$

where:

L_n^j : Phase distance data observed ($\lambda\Phi_n^j$)

B_n^j : Ambiguity phase (λN_n^j) in meter

ρ_n^j : satellite geometry to the receiver

c : Speed of light

- τ_n : receiver time bias
- τ^j : satellite time bias
- Z_n^j : troposphere bias
- I_n^j : ionosphere bias
- ϵ : multipath and noise

The difference between the two observations of the direct (A) and reflected (B) signals from the same satellite produces the following equation:

$$\Delta L_{AB}^j = \Delta \rho_{AB}^j + c\Delta\tau_{AB} + \Delta B_{AB}^j \quad (3)$$

The result of a single difference between the two receivers has receiver bias errors as observed between the master and rover receivers as well as the variation in the level of ambiguity between the two receivers. There is, however, the opportunity to eliminate the receiver time bias and phase ambiguity cycles using the differences from the single difference equation in the two epochs which are written as follows

$$\nabla \Delta L_{AB}^{jk} = \nabla \Delta \rho_{AB}^{jk} + \nabla \Delta B_{AB}^{jk} \quad (4)$$

The distance of the two receivers between the two epochs can be determined using the least-squares method after the variation in the phase distance between them is known. Subsequently, the sea level height determined at the beginning of the measurement can be used as the reference at the next epoch by integration.

2.2 Determination of the distance of the master and rover receivers with GNSS code distance data

There is no need to eliminate the difference in the number of ambiguity cycles with the use of code data. Moreover, using an identical receiver and antenna makes it possible to consider the difference in the receiver bias as zero and this means the variations can be used to propagate the distance between GNSS signals through reflection and direct to determine the distance of the two receivers or the distance of a shadow rover receiver and master receiver.

The use of code data and two identical receivers and antennas with the same model, brand, antenna, and cable length of the antenna to receiver can be used to formulate equation (3) in relation to the vertical distance of the two receivers as follows

$$\Delta P_{rm}^j = \Delta \rho_{rm}^j = h_{rr}^i \sin(\alpha^j) \quad (5)$$

Therefore, the height of the rover receiver from the master is written as follows

$$h_{rr}^i = \frac{\rho_r^j - \rho_m^j}{\sin \alpha} + d \quad (6)$$

α is the elevation angle of the GNSS satellite j as seen from the master receiver while d is the distance of the master from the actual reflecting receiver located just below the master receiver but with the antenna facing down. Meanwhile, there is an opportunity to ignore the d in case it is very small, for example 10 cm, when arranging the antenna height at 20 meters from sea level to anticipate tsunamis reaching more than 15 meters.

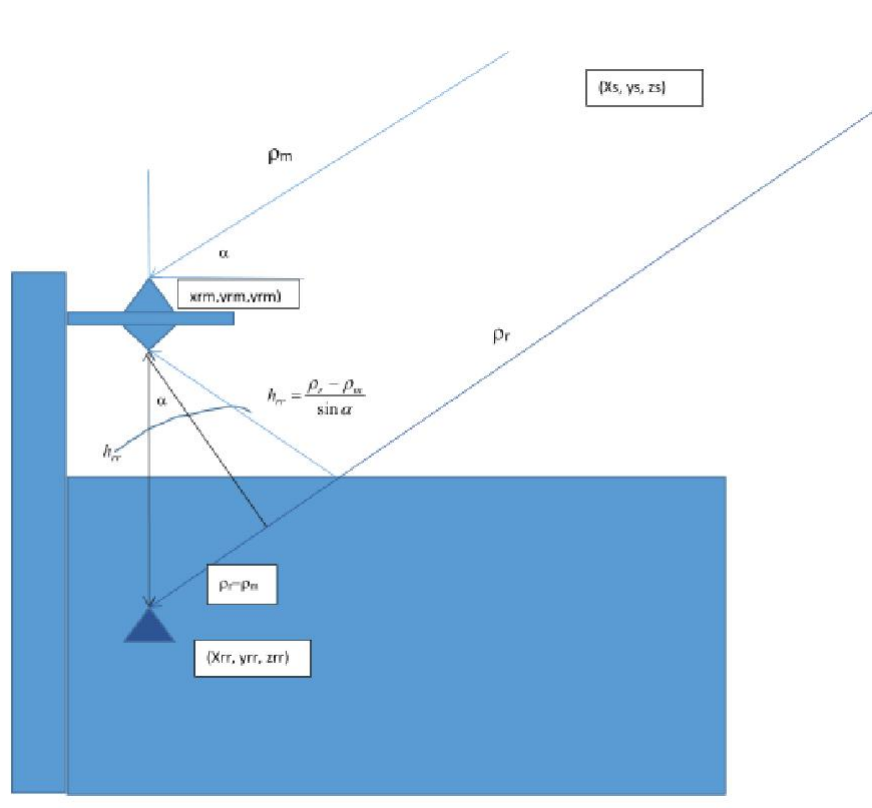


Figure 2. Scenarios for reflection and direct propagation of GNSS signals on shadow and actual rover receivers
The position of the reflected signal receiver is considered to be a shadow rover receiver at

the following depth:

$$h_{rr} = h_{rm} - 20 - 2 \sin\left(\frac{2\pi}{24}t\right) \quad (7)$$

2.3 Simulation Method of GNSS signal reflection data

The process involved in simulating the GNSS signal reflection data is as follows:

- a. Changing ECEF satellite coordinates (x_s, y_s, z_s) to geodetic coordinates (latitude, longitude, altitude (lbh))
- b. Changing the coordinates of the ECEF receiver to lbh
- c. Calculating the satellite elevation angle from the master receiver
- d. Determining the coordinates of the rover receiver in a simulation

The GNSS signal is reflected based on the assumption that it is straight and received by a shadow (pseudo) rover receiver below sea level at an equal distance with the actual receiver to the sea level. In a situation the sea level is undulating with a period of 24 hours and a height of 1 meter which fulfills the sine wave equation,

$$Gal = -\sin\left(\frac{2\pi}{24}t\right) \quad (8)$$

then the height of the hrr shadow rover receiver can be calculated using equation (7).

The latitude and longitude coordinates of the shadow receiver are also the same as those of the master receiver. In this case, the sea level height from the master receiver is half the distance of the shadow rover receiver to the master receiver, which is $h_{al} = 0.5h_{rr}$

- e. Calculating satellite distance to the master receiver using the following relationship:

$$R_{rm}^j = \sqrt{(x_s^j - x_{rm})^2 + (y_s^j - y_{rm})^2 + (z_s^j - z_{rm})^2} \quad (9)$$

- f. Calculating satellite distance to the shadow rover receiver using the following equation:

$$R_{rr}^j = \sqrt{(x_s^j - x_{rr})^2 + (y_s^j - y_{rr})^2 + (z_s^j - z_{rr})^2} \quad (10)$$

- g. Simulating the data on satellite distance to the rover receiver which is identical to the direct signal received in the shadow in such a way it is assumed to be below the sea level receiving the direct signal even though it is above receiving the signal reflected by the seawater. The distance of the satellite received at the rover receiver is proportional to the comparison of its distance with the master receiver, which can be written as follows

$$\rho_r^j = \frac{R_{rr}^j}{R_{rm}^j} \rho_m^j \quad (11)$$

- h. Calculating the distance of the shadow rover from the master receiver from the GNSS signal reflection data using formula (6)

In case the d is assumed to be very small, geometrically, the distance between the rover and master receivers is as follows:

$$h_{rre}^j = \left(\frac{\rho_r^j - \rho_m^j}{\sin \alpha} \right) \quad (12)$$

- i. Calculating the height of sea level from the master receiver

The sea level height is half the distance of the rover from the master receiver and this is indicated in the following equation

$$h_{al}^j = \frac{1}{2} h_{rre}^j \quad (13)$$

- j. Calculating the average sea level height from the master

Wave height is measured from the average sea level height per day. Therefore, the estimated sea level height needs to be averaged as follows:

$$h_{alrat}^j = \frac{1}{N} \sum_{t=0}^{t=N} h_{alrat}^j \quad (14)$$

- k. Calculating sea wave height using the following equation

$$g_{ale}^j = h_{ale}^j - h_{alrar}^j \quad (15)$$

l. The actual sea wave height from the simulation is defined as follows

$$g_{al} = h_{rrm} - h_{rmmrat} \quad (16)$$

m. Estimation error of sea level height

The estimation error of sea level height from GNSS signal reflection data was calculated using the following relationship

$$\delta_{gale} = g_{ale}^j - g_{al} \quad (17)$$

The simulation method to calculate the sea waves from GNSS signal reflection data is shown in the following diagram.

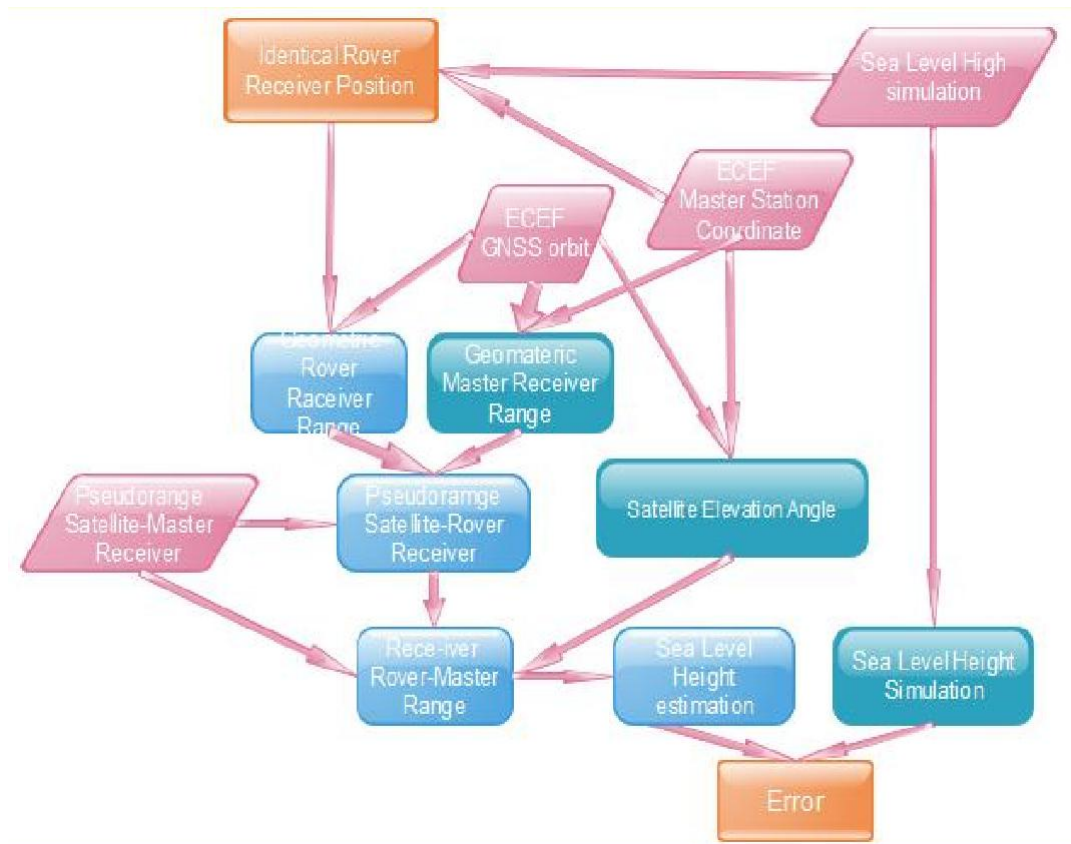


Figure 3. Methodology for estimating sea level height with the pseudo distance of GNSS signal code

3. RESULT AND DISCUSSION

Figure 4 shows a simulation of sea waves where the x-axis is UT and the y-axis is the sea wave height in meters. In this simulation graph, the waves experienced tides with a minimum value at 06:00 UT which corresponds with equation (10) at a period of 24 hours and an amplitude of 1 meter. Moreover, the minimum wave value due to the simulation equation at 06:00 is negative.

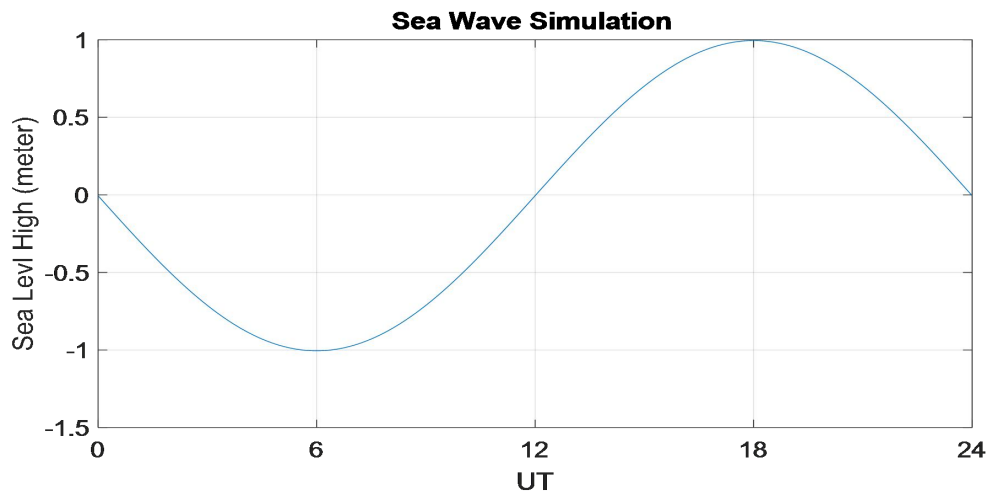


Figure 4. Simulation of sea waves

The sea waves shown in Figure 4 make the reflected signal pass through a distance which is proportional to the fluctuation of the sea wave height. Moreover, the total distance of the GPS signal reflected by the sea from the satellite to the reflected signal receiver is identical to the distance of the GPS satellite signal to the shadow rover receiver as shown in Figure 2. Therefore, the shadow receiver also seems to move periodically like sea waves but with twice the amplitude and at twice the distance for the actual reflected signal receiver above sea level. This means the rover receiver position is at the same latitude and longitude with the master receiver but at the height, as formulated in equation (9), which is shown in Figure 5.

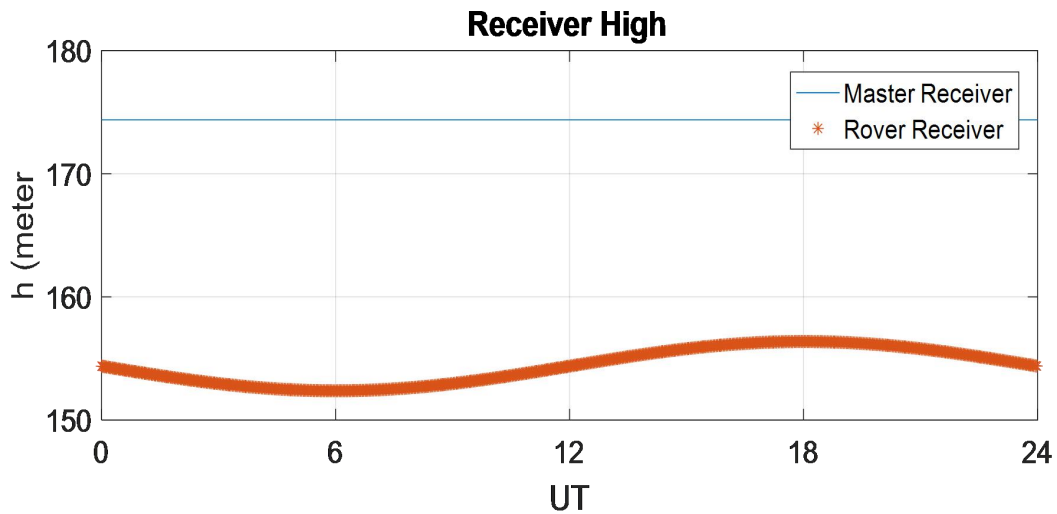


Figure 5. The height of the JOG2 master receiver is shown in the top graph while the shadow rover receiver is presented at the bottom graph in the simulation of signal reflection from GPS satellite No. 9 received just below the master receiver after experiencing reflections by sea level.

The geometry distance between the two receivers to the GPS satellite from their coordinates can be calculated using equations (10) and (11). Subsequently, it is possible to simulate the observation distance for the GPS satellites to the rover receiver with the code distance data received by the master receiver as shown in Figure 6 by multiplying it with the comparison of the geometric distance between the receivers using equation (12) and the results for satellite number 9 shown in Figure 7.

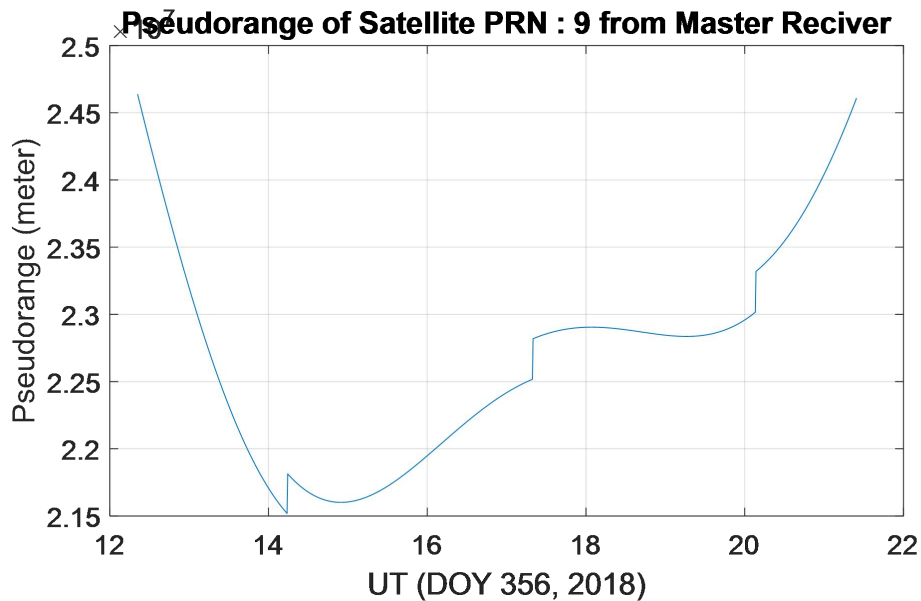


Figure 6. Satellite distance No 9 to Master Receiver

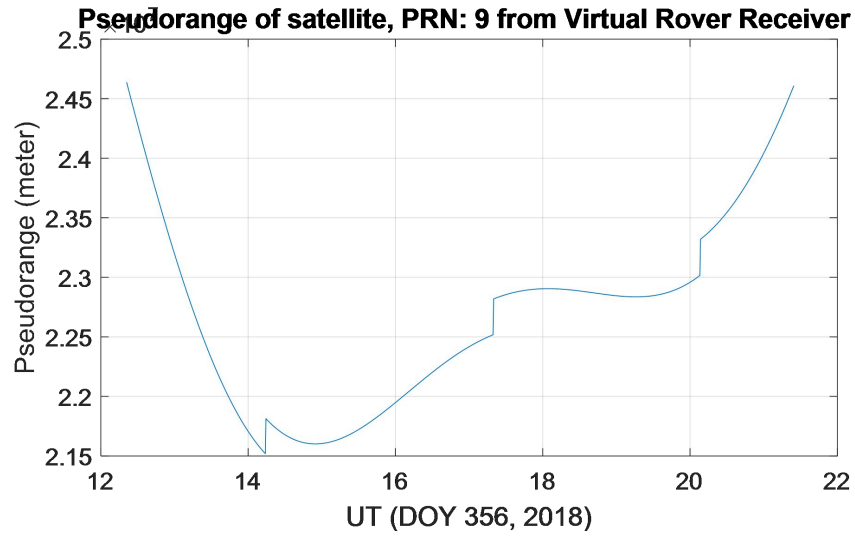


Figure 7. Pseudo Distance of Satellite No 9 to Virtual Rover Receiver

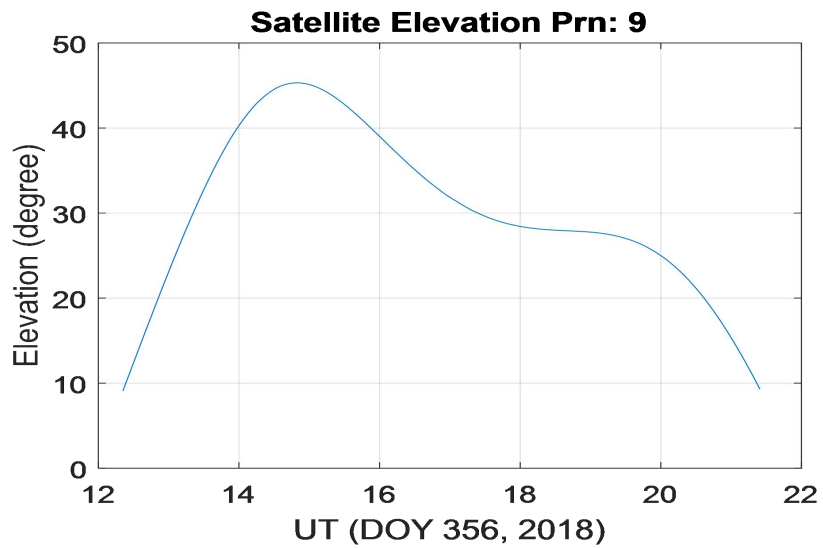


Figure 8. Elevation Satellite No 9

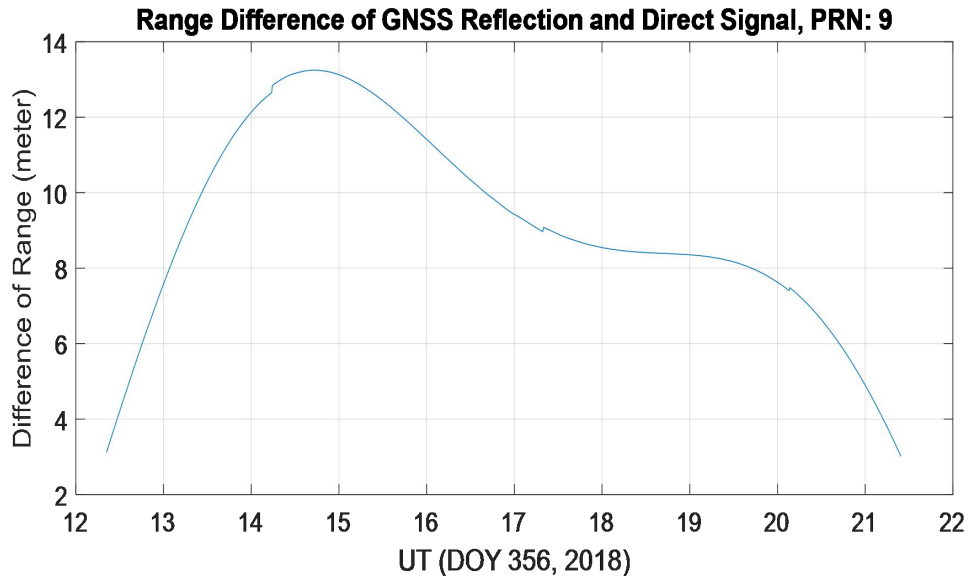


Figure 9. The difference in the observation distance of reflected and direct signals

Figure 9 shows the difference in the observation distance for the reflected and direct signals increased in between UT 12 to 15 with the mileage height almost close to 14 and, subsequently, decreased after experiencing stable conditions between 18 and 19. This is consistent with the elevation angle shown in Figure 8.

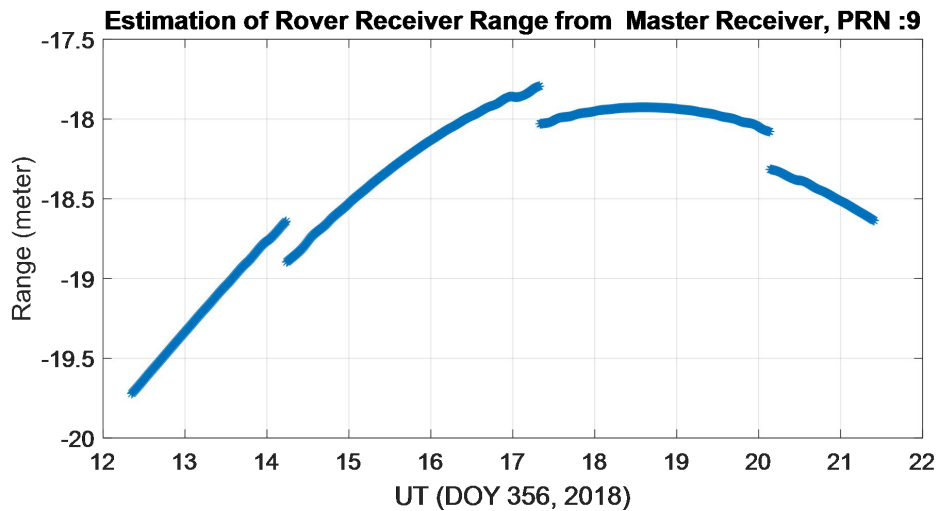


Figure 10. Estimated distance of rover receiver (shadow) from master receiver

Figure 10 shows the estimated distance of the rover receiver or shadow from the master receiver using equation (13) increased in between UT 12 and 19 and, subsequently, decreased at 19 to 22. The distance is negative and this means the rover is positioned under the master.

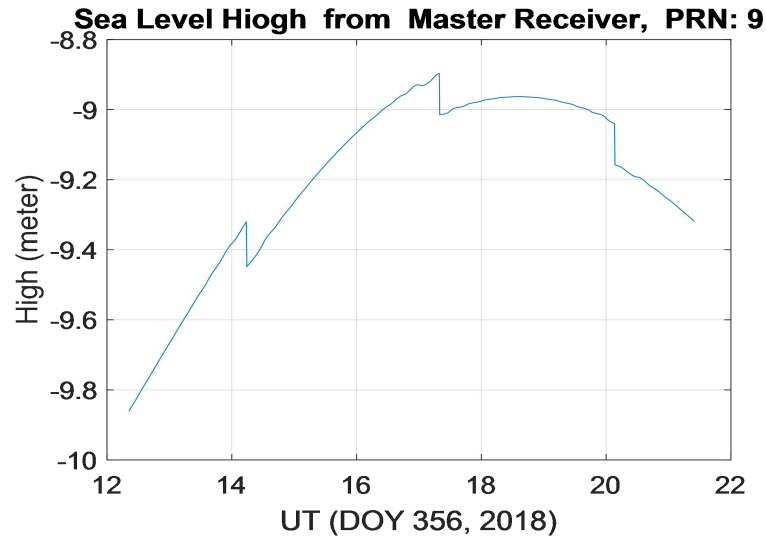


Figure 11. Height of sea level from the master receiver

Figure 11 shows the height of the sea level from the master receiver increased between 12 to 18 and later decreased.

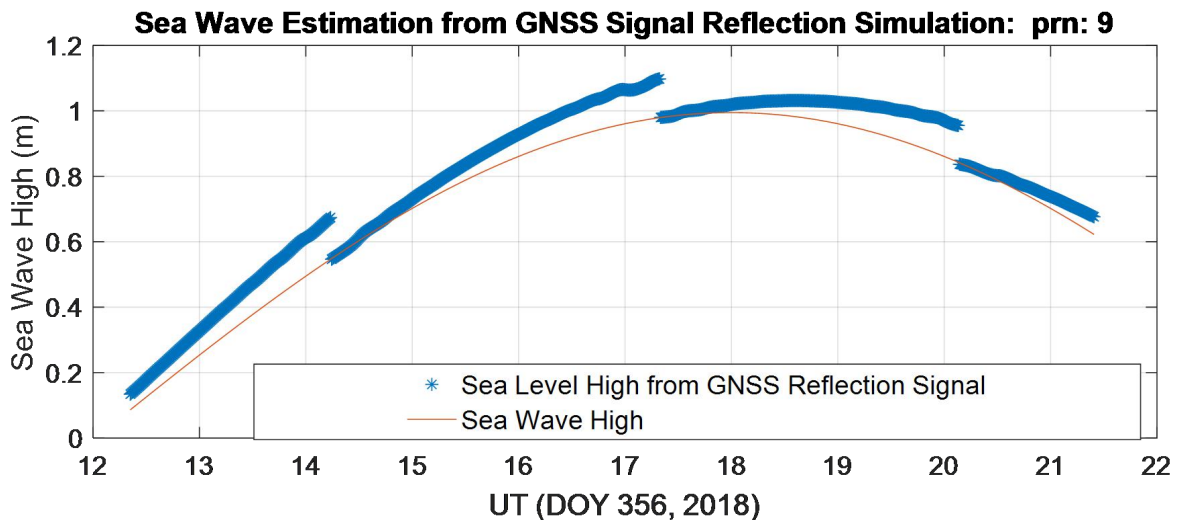


Figure 12. Simulation of determining sea wave height with GNSS

The sea wave height was estimated using equation (16) as shown in Figure 12 and the comparison with the simulated value was also recorded.

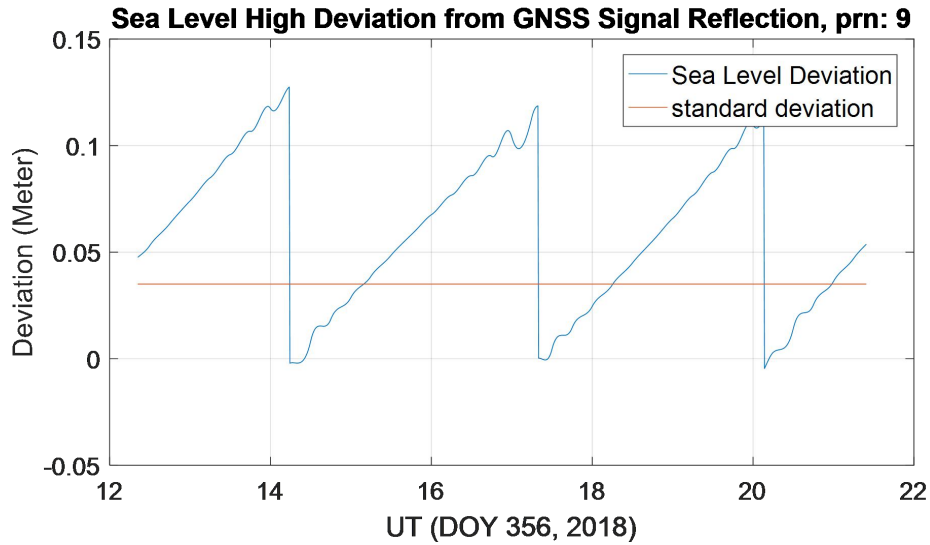


Figure 13. Deviation of sea wave height from a GNSS signal

Figure 13 shows the relative and standard deviations of sea wave height estimated from simulating the wave height in the reflection and direct data of GPS signal on satellite no. 9.

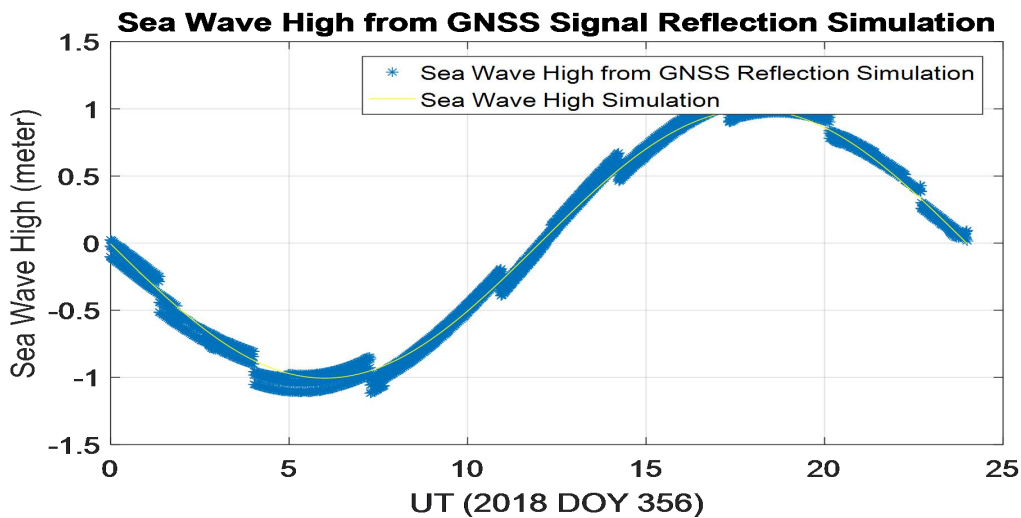


Figure 14. Wave height from the simulation of GNSS JOG2 signal reflection

All the GPS signal reflections observed to estimate the sea wave height were combined to generated a value for 24 hours as shown in Figure 14.

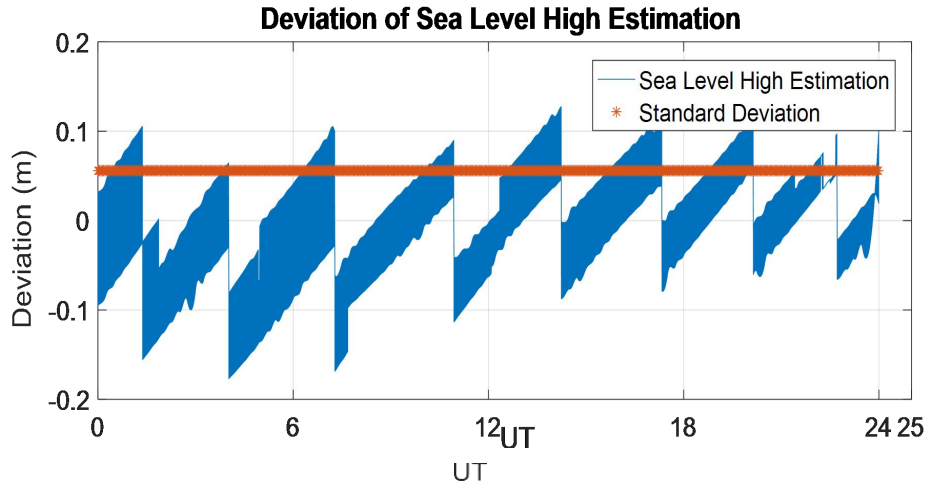


Figure 15. Deviation of estimated sea wave height from P1 code distance data

The relative deviation of the estimated sea wave heights shown in Figure 15 was 0.17 meters while the standard deviation was estimated at 0.056 meters. Therefore, based on simulations, the code distance of GPS signal reflections is suitable to monitor sea wave heights and tsunamis.

4.CONCLUSIONS

The simulations of GNSS signal reflection showed the possibility of using the pseudo distance from the GPS code data to determine sea level height with an accuracy of a few centimeters and this means it is feasible to be used in tidal and tsunami monitoring. The process, however, requires the two receivers are identical with the same length and type of antennas in order to ignore the bias using a single differential on the same satellite received on the receivers.

Acknowledgment

This research was funded through the INSINAS program of the Indonesian Ministry of research technology and higher education with contract No. 14/INS-1/PPK/E4/2020 which has been amended to be No. 70/iNS-1/PPK/E4/2020. And we gratefully thank the Indonesian Geospatial information agency for support in the preparation GNSS real time data. Also, Well deserved recognition is due to Joni Efendi for his consultations and suggestions for using GNSS RTCM data for real time TEC purposes.

REFERENCES

- Artru J, Ducic V, Kanamori H, Lognonné P and Murakami M (2005), Ionospheric detection of gravity waves induced by tsunamis, *Geophys. J. Int*, 160 840-48.
- Chen, C., C., Gao, S., and Maqsoos, M. (2012). Antennas for Global Navigation Satellite System Receivers. 10.1002.
- Garrison, J.L.; Katzberg, S.J.; Hill, M.I. Effect of sea roughness on bistatically scattered range coded signals from the Global Positioning System. *Geophys. Res. Lett.* 1998, 25, 2257–2260. [CrossRef].
- Harijono, S.W.B., Harjadi, P., Fauzi . (2010). InaTEWS (Indonesia Tsunami Early Warning System) : Konsep dan Implementasi. Badan Meteorologi Klimatologi dan Geofisika (BMKG).
- Jin, S.; Cardellach, E.; Xie, F. *GNSS Remote Sensing: Theory, Methods and Applications*; Springer: Dordrecht, The Netherlands, 2014; p. 276.
- Lofgren, J., S., and Haas, R (2014). Sea level measurements using multi-frequency GPS and GLONASS observations. *EURASIP Journal on Advances in Signal Processing*, 2014 50.
- Martin-Neira, M. A passive reflectometry and interferometry system (PARIS): Application to ocean altimetry. *ESA J.* 1993, 17, 331–355.
- Muslim, B., Kumalasari, C, J., Chiuman, N., and Arafah, M, I, F, (2019). Study of GNSS reflection application for monitoring of sea water level. *Komunikasi Fisika Indonesia*.
- Peltier ,W.R. & Hines, C.O., 1976. On the possible detection of tsunamis by a monitoring of the ionosphere, *J. geophys. Res.*, 81(12), 1995–2000.
- R. H. Stewart, “Introduction To Physical Oceanography,” *Am. J. Phys.*, 2008.
- Rudenko, S., Esselborn, S., Schone, T., and Dettmering, D (2019). Impact of terrestrial reference frame realizations on altimetry satellite orbit quality and global and regional sea level trends: a switch from ITRF2008 to ITRF2014. *Solid Earth*, 10, 293-305.
- Semmling, A. M; Schmidt, T ; Wickert, J, dkk, ‘On the retrieval of the specular reflection in GNSS carrier observations for ocean altimetry’, *Radio Science*, Vol:47, RS6007, doi:10.1029/2012RS005007, 2012.
- Zavorotny, V.U.; Gleason, S.; Cardellach, E.; Camps, A. Tutorial on remote sensing using GNSS bistatic radar of opportunity. *IEEE Geosci. Remote Sens. Mag.* 2014, 2, 8–45. [CrossRef].